nature communications

Article

https://doi.org/10.1038/s41467-025-57322-7

Experimental consequences of disorder at an antiferromagnetic quantum phase transition

Received: 9 July 2024

Accepted: 18 February 2025

Published online: 04 March 2025

Check for updates

S. L. Armstrong, D. M. Silevitch & T. F. Rosenbaum

Disorder is known to have a profound influence on classical phase transitions, and it is anticipated to be even more important for quantum phase transitions. However, experimental investigation of the influence of disorder on phase transitions normally requires numerous samples over the range of disorder. Here, we investigate the field-driven quantum phase transition in the antiferromagnet $LiErF_4$. The isotopic distribution of natural Er permits us to probe the transition in the clean and dirty regimes in the same sample. ^{167}Er, with non-zero nuclear spin on 23% of the Er sites, induces random mass disorder in the dirty (low-temperature) regime. We use specific heat and ac magnetic susceptibility experiments to identify a crossover between the two regimes at $T = 150$ mK. The critical behavior is consistent with a violation of the Harris criterion in the clean regime and a change of universality class in the dirty regime.

The introduction of disorder can have many effects on a classical phase transition[1], including altering the universality class of a continuous transition[2], converting a transition from first to second order[3], and even changing the ground state of the system[4]. Quantum phase transitions (QPT)s are expected to be affected more profoundly by disorder, with consequences for both the static and dynamical behavior[5,6]. When a d-dimensional quantum system is mapped to a $(d+z)$ dimensional classical system, where z is the dynamical critical exponent, quenched disorder becomes correlated in the imaginary time dimension. However, systematic approaches to characterizing this hypersensitivity to disorder at a QPT pose distinct theoretical and experimental challenges.

A thorough experimental investigation of the role of disorder in phase transitions requires probing the system at various strengths of that disorder. Typically, randomness is introduced by a structural or compositional mechanism that entails studying a sequence of separate samples over a range of disorder, which can be difficult to synthesize controllably. Here, we adopt an alternate approach by investigating an erbium-based quantum magnet with quenched disorder provided by isotopic variation. Er-167, at 23% natural abundance, is the only stable isotope with non-zero nuclear spin. The energy scale of the hyperfine coupling makes it possible to vary the influence of the quenched disorder simply by changing the temperature.

$LiErF_4$ is an insulating tetragonal crystal with four erbium ions per unit cell (Fig. 1 top). Erbium's 4f electrons ($J = 15/2$) provide large localized moments that are dipolar-coupled. The electronic ground state of an erbium ion is a Kramers doublet with a 26 K energy gap to its first excited state. This subspace can be treated as an effective spin-½ system. The crystal field induces strong easy plane anisotropy which, within the effective subspace, is fully described by an anisotropic g-factor $(g_\perp / g_\parallel)^2 = 13.8$. In-plane anisotropy, originating from order by disorder, causes the moments to point along the a or b-axis[7]. These symmetries correspond to the XY/h_4 universality class.

$LiErF_4$ orders antiferromagnetically[8] with a bilayer structure at $T_N = 373(5)$ mK[7]. The observed T_N is approximately half of mean-field predictions, and its critical exponents have been reported as $\beta = 0.15(2)$ and $\alpha = -0.28(4)$. These exponents are consistent with a 2D quasi-Ising description where the exponents lie in a universal window bounded by the exponents of the 2D Ising ($\beta = 0.125$) and XY ($\beta = 0.23$) models. The strength of the in-plane anisotropy tunes between these bounds[9]. This reduction in dimensionality is surprising for a material whose 2D nature is not evident from its structure; however, it has been observed in similar materials[10].

A QPT to a paramagnetic state is induced by applying a magnetic field of order 4 kOe along the c-axis (Fig. 1 bottom). $\beta_H = 0.31(2)$ was reported for this QPT which is near the values of both the 3D Ising ($\beta_H = 0.3265(3)$) and XY ($\beta_H = 0.349(2)$) models. This agrees with a $d+1$

Division of Physics, Mathematics, and Astronomy, California Institute of Technology, Pasadena, CA 91125, USA. e-mail: tfr@caltech.edu

https://doi.org/10.1038/s41467-025-57322-7

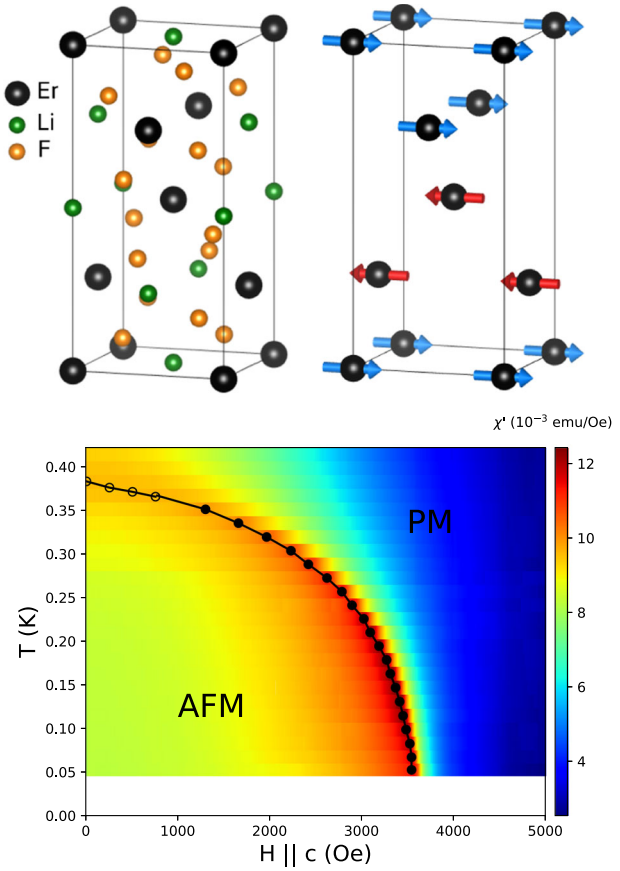

Fig. 1 | Structure and magnetism of $LiErF_4$. (top left) Body-centered tetragonal unit cell of $LiErF_4$. Lattice constants are $a = 5.162$ Å (horizontal), $c = 10.70$ Å (vertical). Er, Li, and F sites are represented as black, green, and orange spheres, respectively. (top right) Arrows on the Er sites represent the double layer antiferromagnetic spin structure of the ordered state. (bottom) The data points mark the measured phase diagram as a function of temperature and c-axis magnetic field, obtained by sweeping temperature (open circles) and field (filled circles). T_N and H_c are defined by the maximum in susceptibility for a given temperature and field sweep, respectively. Imagemap shows the susceptibility data from Fig. 2.

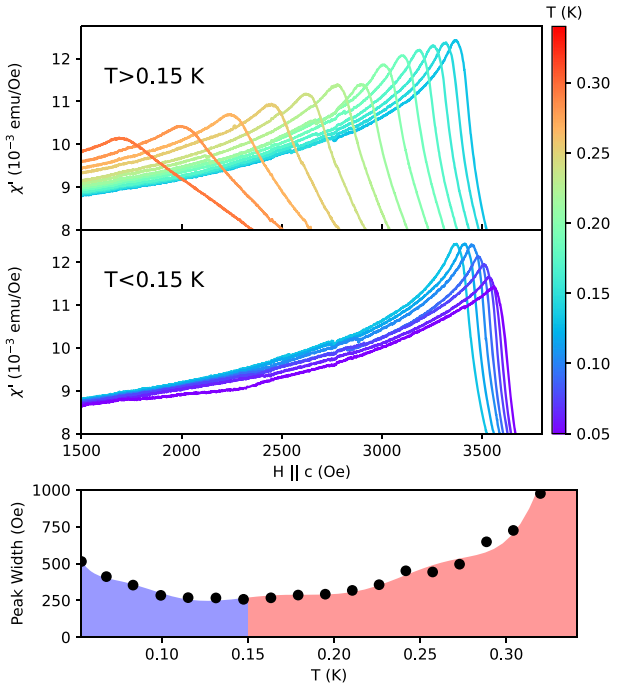

Fig. 2 | Ac magnetic susceptibility of $LiErF_4$. 0.5 Oe drive field and 10 kHz frequency vs. c-axis magnetic field at a series of fixed temperatures above (top) and below (middle) $T = 150$ mK. (bottom) Width of the peak at 90% of its maximum value. Red and blue shading identify the high and low temperature regimes, respectively.

mapping from the classical phase transition. Mean field calculations of the critical field are sensitive to which crystal field parameters are used; values ranging from 5.75 kOe[7] to 9.5 kOe[11] have been reported. However, all calculations overestimate the experimentally observed critical field, H_c, and along with the dimensional reduction and the non-mean field critical exponents, point to the role of spin fluctuations at the transition.

For erbium sites occupied by Er-167 atoms, the nuclear moment (I = 7/2) couples antiferromagnetically to the electronic moment. A coupling strength of $A_{hf} = 6$ mK was found by electron-paramagnetic-resonance spectroscopy[12]. This coupling splits the Kramers doublet into a multiplet. At the level of a single ion calculation, these states have a span of 160 mK (see Fig. S2). In $LiHoF_4$, an Ising ferromagnet within the same family of materials, the hyperfine coupling slaves the nuclear spins to the electronic spins at sufficiently low temperature, increasing the critical field[13] and allowing a new class of low energy, electronuclear excitations[14], but does not alter its universality class[15]. The increase in H_c is a general effect due to a reduction in effective field felt by the electronic spins[16]. Since Ho has only one stable isotope, no disorder is introduced by the nuclear moment.

Mean field calculations on $LiErF_4$ that include nuclear moments on 23% of sites find a similar increase in H_c of ~500 Oe[7,11]. The choice of crystal field parameters does not strongly impact the change in H_c. Since the nuclear spin locks with the electronic spin, the local XY/h_4 symmetry of the system is unbroken by the disorder and belongs to the category of random mass (also referred to as random-T_c) disorder[1]. Random field disorder is a stronger form of disorder which breaks the local symmetry. Previous work on $LiErF_4$ examined the effect of random-field disorder by substituting Er with Ho and found a reentrant glassy state with 6% substitution[17].

Results

We plot in Fig. 2 field sweeps of the ac magnetic susceptibility in the linear and zero-frequency limits along the c-axis on a needle crystal with dimensions (0.35 x 0.35 x 1.65 mm^3) at a series of temperatures. A critical field of $H_c(T = 0) = 3645(6)$ Oe is found by fitting the phase boundary to a power law form. This field is 10% lower than a reported value of $H_c(T = 0) = 4000$ Oe[7]. We attribute this discrepancy to demagnetization effects (see Methods). At temperatures above 150 mK (Fig. 2 top), we observe steadily increasing critical divergence as the temperature drops, corresponding to the diminishing strength of thermal fluctuations. Below 150 mK (Fig. 2 middle), the opposite trend is observed: the sharpness of the transition is reduced continuously as the temperature decreases. This evolution in the shape of the divergence can be parameterized by the full width of the peak at 90% of its maximum for each T (Fig. 2 bottom). This heuristic metric reinforces the trend apparent in the raw data of two qualitatively distinct regimes separated at $T = 150$ mK. In a conventional description of a QPT with a single energy scale, monotonic thermal broadening is expected and can be understood as a finite size effect in the imaginary time dimension[18]. The unexpected broadening in the low temperature regime suggests the presence of a second energy scale that is not electronic in origin. To check for the possibility of glassy dynamics, we performed 3 GHz susceptibility measurements using a microwave loop gap resonator[19] on a sample cut from the same parent sample. We found qualitatively similar behavior, narrowing and then broadening of the peak in the susceptibility below $T \sim 150$ mK, with no observable alteration to $H_c(T)$ (see Fig. S1). Similar glassy materials have far

https://doi.org/10.1038/s41467-025-57322-7

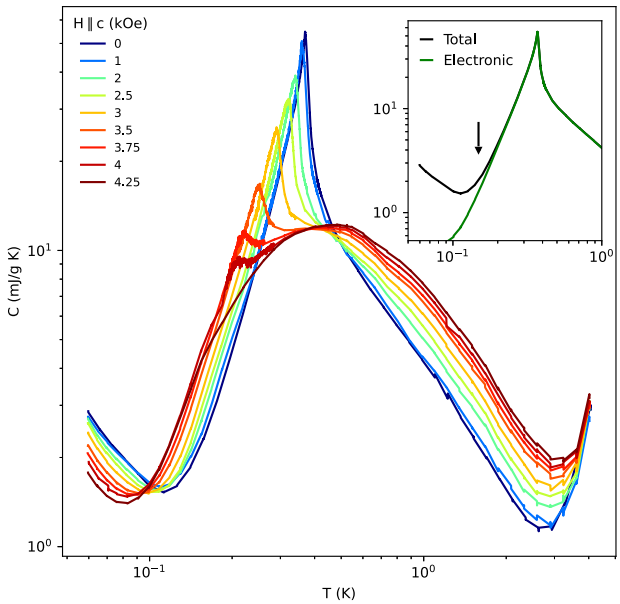

Fig. 3 | Specific heat vs. temperature for a series of magnetic fields along the *c*-axis. (inset) Total and purely electronic heat capacities at zero field. Arrow at $T = 150$ mK marks where the disordered nuclear spin bath couples to the electronic spins.

stronger frequency dependence in their freezing temperature: $\frac{\Delta T_F}{T_F \Delta \log_{10}(f)} \sim 0.08$[17]. A six-decade increase in frequency should correspond to an increase in H_c ~ 59%. The absence of variation in H_c argues against a reentrant transition to a spin glass state.

To elucidate the nature of the $T \to 0$ behavior, we measured the specific heat, *C(T,H)*, on a single-crystal thin plate (1 x 1 x 0.04 mm^3) of $LiErF_4$ (Fig. 3). Data was collected over a temperature range of 0.058 K to 4 K and at fields parallel to *c* up to 4.25 kOe. These measurements were taken to lower temperatures and higher fields than previously reported[7,20], and allow us to fully characterize the specific heat through the QPT. Within this temperature range, contributions from phonons are negligible[7].

The high-*T* upturn in *C(T)* is due to the crystal field splitting and is negligible in the temperature range of the magnetic ordering. The peak at the ordering transition is well described by a power law of the form:

$$C(T) = A^{+/-}\left|\frac{T - T_N}{T_N}\right|^{-\alpha} + D \tag{1}$$

where *A*+ and *A*− are the amplitudes in the paramagnetic and antiferromagnetic states, respectively, and *D* is a non-critical background. We find that the specific heat exponent agrees within error of the previously reported value $\alpha = -0.28(4)$[7]. As seen in Fig. 3, at the lowest temperatures there is an additional upturn in the specific heat, attributable to a Schottky contribution[20]. The Schottky anomaly occurs when the coupling between nuclear and electronic spins begins to dominate over thermal fluctuations. We account for the Schottky contribution by assuming the standard T^{-2} high-temperature form[21]. This allows us to subtract off the Schottky contribution to the specific heat and isolate the purely electronic contribution (Fig. 3 inset). The electronic and total heat capacities begin to separate at 150 mK, coincident with the broadening of the divergence of the magnetic susceptibility, pointing to the naturally occurring isotopic abundance as the relevant source of disorder. Furthermore, an integration of the electronic specific heat gives entropy $S = R$ ln(2) for all fields (see Fig. S3). The lack of excess entropy rules out a more exotic ground state, such as a quantum spin liquid, as a source of the broadening.

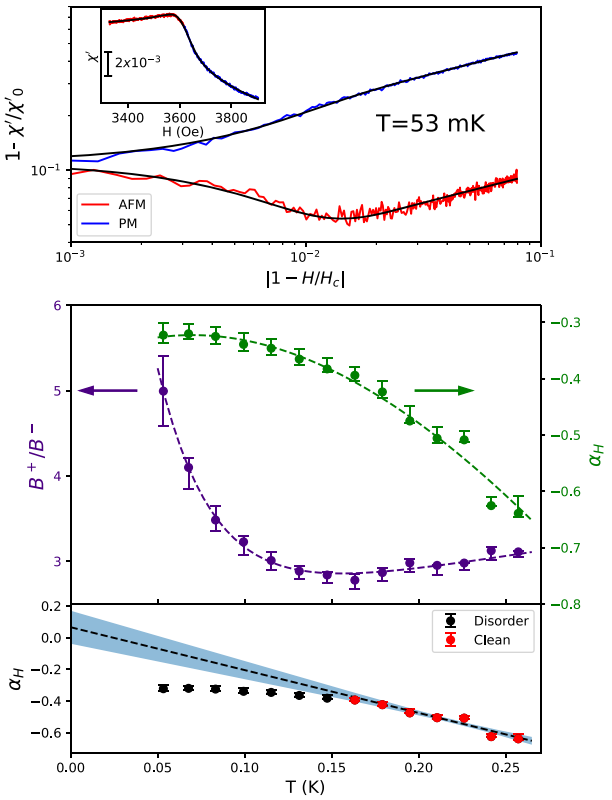

Fig. 4 | Critical behavior of the ac susceptibility of $LiErF_4$ in the paramagnet (PM) and antiferromagnet (AFM). (top) Susceptibility at $T = 53$ mK (black) and fits to a critical divergence form with Gaussian field broadening (see text for details). Red and blue denote $H < H_c$ and $H > H_c$, respectively. (inset) Susceptibility vs magnetic field at $T = 53$ mK. The scale bar marks absolute units of emu/Oe. The data is well described by a pure power law over 0.8 decades. Near the transition, deviations from linearity occur due to the Gaussian convolution. (middle) Temperature dependence of the amplitude ratio and critical exponent describing the control parameter susceptibility and a transition between universality classes. Error bars are estimated by refitting with a fit range varied by ±5% of a decade. (bottom) Critical field exponent replotted, showing a linear extrapolation to $T = 0$ of the data in the clean, high-temperature limit (red points). Shaded region shows the 1σ error band of the extrapolation.

We present in Fig. 4 a power law analysis of the susceptibility field sweeps to probe the low-temperature critical behavior. The order parameter of an antiferromagnet is the staggered magnetization, and the critical behavior of the susceptibility along the *c*-axis does not correspond to a conventional γ exponent. However, it can be understood under the general theory of critical scaling at QPTs developed by Belitz and Kirkpatrick[22]. In this framework, a "control-parameter susceptibility" is defined as

$$\chi_r = -\frac{\partial^2 f}{\partial r^2} \tag{2}$$

where *f* is the free energy and *r* is the athermal tuning parameter that induces the QPT. Two critical exponents are defined for this susceptibility: one at zero temperature as a function of field,

$$\chi_r(H, T = 0) = B^{+/-}\left(\left|\frac{H - H_c}{H_c}\right|\right)^{-\alpha_H} + \chi_0 \tag{3}$$

and the other at $H = H_c$ as a function of temperature,

$$\chi_r(H = H_c, T) = aT^{-\alpha_T} \tag{4}$$

where $B+$ and $B-$ are the amplitudes in the paramagnetic and antiferromagnetic states, respectively, χ_0 is a non-critical background, and a is the amplitude at the critical field. Here the notation α is used because, in the case of $r = T$, the control parameter susceptibility is given by C/T. For a QPT induced by a magnetic field along the c-axis, χ_r corresponds to χ_c, the magnetic susceptibility along the c-axis.

We model a macroscopic distribution of H_cs with width δH_c, most likely arising from demagnetization fields due to shape effects, by convolving the power law with a Gaussian. The convolution allows us to fit the susceptibility through the transition and improves the fit stability of the amplitude and critical exponent[23]. Our fit gives $\delta H_c \sim 30Oe \rightarrow \frac{\delta H_c}{H_c} = 8 \times 10^{-3}$. The data is well fit by this functional form over a range of reduced fields spanning −0.8 to 0.8 for temperatures up to at least 273 mK. The error in the fit parameters is dominated by the systematic error associated with the fit range. At high temperatures, α_H increases rapidly as temperature decreases. It begins to saturate at $T \sim 150$ mK and reaches $\alpha_H = -0.32(2)$ in the $T \rightarrow 0$ limit. The amplitude ratio B^+/B^- begins to increase at 150 mK and captures the same behavior as the heuristic width metric in Fig. 2. At our base temperature of 53 mK, B^+/B^- has not saturated, but we can establish a lower bound of $B^+/B^- > 5$ at $T = 0$.

Discussion

The amplitude ratio, B^+/B^-, typically marks a particular universality class[24]. The rapid increase in the ratio at low temperatures indicates that the universality class changes as the nuclear and electronic spins lock. Further evidence that the change in amplitude ratio is due to the nuclear spins is seen in a comparison between field sweeps taken on $LiErF_4$ samples with a natural isotopic abundance and with isotopically pure erbium-168[25]. The isotopically pure sample has a much sharper peak than the natural sample at 35 mK, reaffirming the role of nuclear spins.

The Harris criterion $d\nu > 2$ is a necessary condition for a universality class to be unchanged by random mass disorder, where ν is the critical exponent of the correlation length[26,27]. The Harris criterion determines if the correlation length grows rapidly enough for the effective strength of disorder to go to zero at the transition. Since only dimensions with random disorder contribute to the Harris criterion, QPTs obey $d\nu > 2$ rather than (d+z)ν > 2. Hence QPTs require a larger ν relative to an analogous classical transition as a manifestation of their sensitivity to disorder[1]. Since the isotopic disorder in our system does not break local symmetry, it falls within the category of random mass disorder, and the Harris criterion is applicable.

Given that β_H is far from the mean field value ($\beta_{MF} = 0.5$) and that mean field calculations overestimate H_c, we assume that the dimensionality of the system is below its upper critical dimension and that a hyperscaling relation is valid. Under this assumption, we can express the Harris criterion in terms of the critical exponents of the control parameter susceptibility using Eqs. 2.23a and 2.23b of Belitz and Kirkpatrick[22]:

$$d\nu = \frac{2\alpha_T - \alpha_H(1+\alpha_T)}{\alpha_T} > 2 \tag{5}$$

When $\alpha_T > 0$, this inequality can be simplified to

$$\alpha_H < 0,$$

which is analogous to the standard form of the Harris criterion expressed in terms of the classical critical exponent, $\alpha < 0$. The Harris criterion pertains to the critical exponents of clean systems. Since α_T remains positive in both the clean and disordered universality classes[7], we can focus solely on the sign of α_H in the clean universality class to determine the validity of the Harris criterion in the present measurements. The rapid change of α_H in the clean regime is cut off by the disorder and prevents us from definitively characterizing α_H^{clean} in the zero-temperature limit. A linear extrapolation of the clean regime to $T = 0$ finds $\alpha_H^{clean} = 0.06(10)$, (see Fig. 4) which is consistent within error bars with a specific heat exponent for both the classical 3D Ising ($\alpha = 0.110(1)$) and 3D XY ($\alpha = -0.015(1)$) models. However, a change in universality implies that the Harris criterion was violated, $\alpha_H^{clean} > 0$ at $T = 0$, and the operative universality class is classical 3D Ising. The critical exponents of all universality classes with a finite effective disorder strength at a phase transition follow the Chayes-Chayes-Fisher-Spencer relation $d\nu^{disorder} > 2$[28]. This relation differs from the Harris criterion in that it uses the critical exponents of the disordered universality class. We find that our disordered universality class is consistent with this relation because $\alpha_H^{disorder} < 0$.

In conclusion, magnetic susceptibility and specific heat measurements reveal that the QPT in antiferromagnetic $LiErF_4$ is affected profoundly by naturally-occurring isotopic disorder. At temperatures below 150 mK, nuclear spins slave to electronic spins, reducing the effective field and introducing random mass disorder. We identify χ_c as a relevant observable to study the critical behavior of a field-induced QPT and relate its critical exponents to the Harris criterion and the Chayes-Chayes-Fisher-Spencer relation. Our data is consistent with a violation of the Harris criterion in the clean high-temperature regime, above the energy scale of the hyperfine coupling, and a change in universality class when disorder becomes manifest at low T. The critical exponents of the disordered universality class obey the Chayes-Chayes-Fisher-Spencer relation.

The unconventional power behavior of the susceptibility in the disordered universality class that characterizes $LiErF_4$ may well point to Griffiths physics and motivates further studies of the paramagnetic regime (see Supplementary Note for further discussion). More generally, nuclear moments present a well-characterized platform to manipulate disorder in situ, with sensitivity to temperature and magnetic field, and potential tunability of the low-T electronuclear spectrum itself.

Methods

Sample

Two parent single crystal samples were obtained from commercial sources. T_N at zero field was used to determine sample quality. Susceptibility measurements found sample 1 and sample 2 had T_N 's of 379 mK and 349 mK, respectively. Hence sample 1 was used for susceptibility, specific heat, and microwave measurements, while sample 2 was characterized with susceptibility measurements for comparison. Measurements in the needle limit (0.35×0.35×1.65 mm^3) and plate limit (3 x 3 x 0.4 mm^3) were made on samples cut from sample 1 to investigate demagnetization effects on H_c. At $T = 53$ mK, H_c was measured as 3560 Oe and 4669 Oe for the needle and plate, respectively. The geometry had no effect on T_N at zero field. Additionally, measurements were made on a needle (1.25 x 1.25 x 6 mm^3) cut from sample 2. An H_c of 3223 Oe was measured at $T = 53$ mK, corresponding to a reduction of ~10% in H_c and T_N relative to sample 1. Broadening was observed at $T = 150$ mK regardless of geometry or parent sample, substantiating the critical role ascribed to nuclear spin disorder.

Susceptibility

Susceptibility measurements were made using a commercial susceptometer (PPMS DR, Quantum Design). Measurements were taken in the linear regime with a drive field of 0.5 Oe and with frequencies of 1 kHz (power law fits) and 10 kHz (phase diagram). No variation in H_c was observed between these frequencies.

Specific heat

Measurements were made on a plate sample (1 x 1 x 0.04 mm^3) cut from sample 1 using a commercial sub-Kelvin calorimeter (PPMS DR, Quantum Design) operating in a standard relaxation mode. Away from the phase boundary, data were taken in discrete steps using

small thermal pulses ($\frac{\Delta T}{T} = 0.02$) fit to a two-tau model. Near the transition, measurements were made with a large pulse, $\frac{\Delta T}{T} = 0.15$, to obtain higher point density, and the specific heat was extracted by analyzing the evolution of the slope of the *T(t)* response of the calorimeter[29].

Data availability

The susceptibility and specific heat data generated in this study have been deposited in the CaltechDATA repository under accession code 10.22002/n13wc-zwc92, available at https://data.caltech.edu/records/n13wc-zwc92.

References

1. Vojta, T. Disorder in Quantum Many-Body Systems. *Annu. Rev. Condens. Matter Phys.* **10**, 233–252 (2019).
2. Pelissetto, A. & Vicari, E. Randomly dilute spin models: A six-loop field-theoretic study. *Phys. Rev. B* **62**, 6393–6409 (2000).
3. Sang, Y., Belitz, D. & Kirkpatrick, T. R. Disorder Dependence of the Ferromagnetic Quantum Phase Transition. *Phys. Rev. Lett.* **113**, 207201 (2014).
4. Alba, M., Hammann, J. & Nogues, M. Phase diagrams of two dilute insulating systems with competing interactions: $CdCr_{2x}In_{2-2x}S_4$ and $ZnCr_{2x}Al_{2-2x}S_4$. *J. Phys. C: Solid State Phys.* **15**, 5441 (1982).
5. Bao, W. et al. Magnetic correlations and quantum criticality in the insulating antiferromagnetic, insulating spin liquid, renormalized Fermi liquid, and metallic antiferromagnetic phases of the Mott system V_2O_3. *Phys. Rev. B* **58**, 12727–12748 (1998).
6. Jaramillo, R., Feng, Y., Wang, J. & Rosenbaum, T. F. Signatures of quantum criticality in pure Cr at high pressure. *Proc. Natl Acad. Sci.* **107**, 13631–13635 (2010).
7. Kraemer, C. et al. Dipolar Antiferromagnetism and Quantum Criticality in $LiErF_4$. *Science* **336**, 1416–1419 (2012).
8. Beauvillain, P., Renard, J.-P. & Hansen, P.-E. Low-temperature magnetic susceptibility of $LiErF_4$: evidence of antiferromagnetic ordering at 0.38 K. *J. Phys. C: Solid State Phys.* **10**, L709 (1977).
9. Taroni, A., Bramwell, S. T. & Holdsworth, P. C. W. Universal window for two-dimensional critical exponents. *J. Phys.: Condens. Matter* **20**, 275233 (2008).
10. Babkevich, P. et al. Dimensional Reduction in Quantum Dipolar Antiferromagnets. *Phys. Rev. Lett.* **116**, 197202 (2016).
11. Babkevich, P. et al. Neutron spectroscopic study of crystal-field excitations and the effect of the crystal field on dipolar magnetism in $LiRF_4$ (*R* = Gd, Ho, Er, Tm, and Yb). *Phys. Rev. B* **92**, 144422 (2015).
12. Sattler, J. P. & Nemarich, J. Electron-Paramagnetic-Resonance Spectra of Nd^{3+}, Dy^{3+}, Er^{3+}, and Yb^{3+} in Lithium Yttrium Fluoride. *Phys. Rev. B* **4**, 1–5 (1971).
13. Bitko, D., Rosenbaum, T. F. & Aeppli, G. Quantum Critical Behavior for a Model Magnet. *Phys. Rev. Lett.* **77**, 940–943 (1996).
14. Libersky, M., McKenzie, R. D., Silevitch, D. M., Stamp, P. C. E. & Rosenbaum, T. F. Direct Observation of Collective Electronuclear Modes about a Quantum Critical Point. *Phys. Rev. Lett.* **127**, 207202 (2021).
15. McKenzie, R. D. & Stamp, P. C. E. Thermodynamics of a quantum Ising system coupled to a spin bath. *Phys. Rev. B* **97**, 214430 (2018).
16. Chakraborty, P. B., Henelius, P., Kjønsberg, H., Sandvik, A. W. & Girvin, S. M. Theory of the magnetic phase diagram of $LiHoF_4$. *Phys. Rev. B* **70**, 144411 (2004).
17. Piatek, J. O. et al. Phase diagram with an enhanced spin-glass region of the mixed Ising–XY magnet $LiHo_xEr_{1-x}F_4$. *Phys. Rev. B* **88**, 014408 (2013).
18. Sondhi, S. L., Girvin, S. M., Carini, J. P. & Shahar, D. Continuous quantum phase transitions. *Rev. Mod. Phys.* **69**, 315–333 (1997).
19. Libersky, M. M., Silevitch, D. M. & Kouki, A. Design of a loop-gap resonator with bimodal uniform fields using finite element analysis. in *2019 22nd International Conference on the Computation of Electromagnetic Fields (COMPUMAG)* 1–4 https://doi.org/10.1109/COMPUMAG45669.2019.9032729 (2019)..
20. Mennenga, G., Jongh, L. J., Huiskamp, W. & Laursen, I. A comparative study of the magnetic ordering specific heats of four S = 1/2 dipolar magnets: $LiRF_4$ (R = Er, Dy, Ho, Tb). *J. MAGN. MAGN. MATER. - J. MAGN MAGN MATER* **44**, 48–58 (1984).
21. Phillips, N. E. Low-temperature heat capacity of metals. *C. R. C. Crit. Rev. Solid State Sci.* **2**, 467–553 (1971).
22. Kirkpatrick, T. R. & Belitz, D. Exponent relations at quantum phase transitions with applications to metallic quantum ferromagnets. *Phys. Rev. B* **91**, 214407 (2015).
23. Wosnitza, J. From Thermodynamically Driven Phase Transitions to Quantum Critical Phenomena. *J. Low. Temp. Phys.* **147**, 249–278 (2007).
24. Pelissetto, A. & Vicari, E. Critical phenomena and renormalization-group theory. *Phys. Rep.* **368**, 549–727 (2002).
25. Nikseresht Ghanepour, N. Classical and Quantum Critical Phenomena in the Dipolar Antiferromagnet $LiErF_4$. (ÉCOLE POLYTECHNIQUE FÉDÉRALE DE LAUSANNE, 2012).
26. Harris, A. B. Effect of random defects on the critical behaviour of Ising models. *J. Phys. C: Solid State Phys.* **7**, 1671–1692 (1974).
27. Brooks, H. A. The 'Harris criterion' lives on. *J. Phys.: Condens. Matter* **28**, 421006 (2016).
28. Chayes, J. T., Chayes, L., Fisher, D. S. & Spencer, T. Finite-Size Scaling and Correlation Lengths for Disordered Systems. *Phys. Rev. Lett.* **57**, 2999–3002 (1986).
29. Riegel, S. & Weber, G. A dual-slope method for specific heat measurements. *J. Phys. E: Sci. Instrum.* **19**, 790–791 (1986).

Acknowledgements

We are grateful to Patrick Lee and Philip Stamp for insightful discussions, Matthew Libersky for technical assistance in obtaining and analyzing microwave data, and Christopher Simon for technical assistance in the single ion calculation. This work was supported by the US Air Force Office of Scientific Research, Grant #FA9550–25-1-0017, DMS and TFR co-PIs.

Author contributions

S.L.A. and D.M.S. conducted the experimental work. S.L.A., D.M.S. and T.F.R. analyzed the data and prepared the manuscript.

Competing interests

The authors declare no competing interests.

Additional information

Supplementary information The online version contains supplementary material available at https://doi.org/10.1038/s41467-025-57322-7.

Correspondence and requests for materials should be addressed to T. F. Rosenbaum.

Peer review information *Nature Communications* thanks the anonymous reviewer(s) for their contribution to the peer review of this work. A peer review file is available.